

ASTROPHYSICS WITH CLOSURE PHASES

J. D. Monnier¹

Abstract. After a brief introduction, this contribution will discuss practical strategies to exploit the unique science potential of closure phases in optical interferometry, especially in the case of only three telescopes when direct imaging is near-impossible. Prototype source morphologies will be investigated in detail (binary and “dust shell + star”), and will illustrate how closure phase measurements can be used both for “Precision Interferometry” as well as qualitatively new probes of circumstellar environments. During this meeting, the notion of a “Closure Differential Phase” came to light, and some interesting properties of this quantity are here introduced.

1 Introduction

The vast majority of all optical interferometry results have been based on measurements of the visibility amplitude alone, the fringe phase information being corrupted by the turbulent atmosphere. With the advent of telescope arrays (three or more telescopes), the *closure phase* can be used to overcome this difficulty and reveal fundamentally new information about the sources under study, the amount of asymmetry in the brightness distribution.

In this chapter, we review the basic principles behind the closure phase and outline practical strategies for designing and subsequently interpreting observations using three-telescope arrays. For simple sources such as binary stars, modelling of the closure phases can be used (theoretically) to reach unprecedented precision in model parameters, truly “Precision Interferometry.” For more complicated objects (such as accretion disks around young stars), the ability to measure even a limited number of closure phases will lead to much astrophysical progress, even before true interferometric “imaging” becomes standard practice. However, this will require a deeper and more subtle understanding of the properties of closure phases than typically employed, and this chapter contains useful ways of thinking about closure phases in some common astrophysical contexts.

¹ Harvard-Smithsonian Center for Astrophysics & University of Michigan Astronomy Department

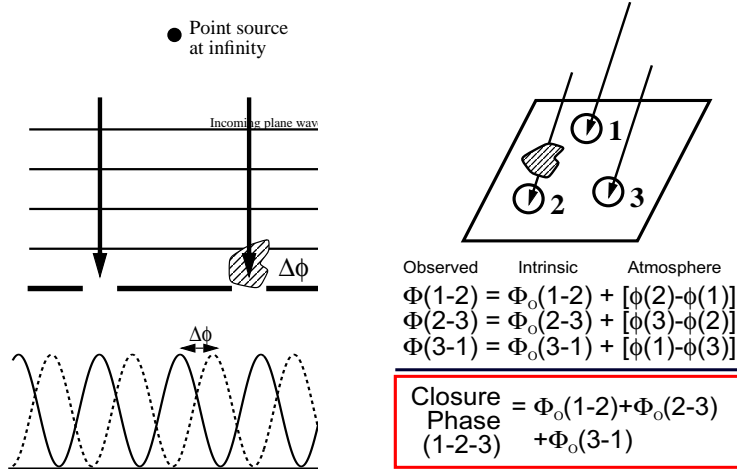


Fig. 1. (*left panel*): In an interferometer, a phase delay above an aperture causes a phase shift in the detected fringe pattern. (*right panel*): Phase errors introduced at any telescope causes equal but opposite phase shifts, canceling out in the *closure phase* (after Readhead *et al.* 1988).

1.1 Motivation

When light from two telescopes i and j are interfered, the complex visibility \tilde{V}_{ij} is derived from the contrast and phase of the resulting fringes. We can see how telescope-specific phase delays caused by atmospheric turbulence (or anything else) affect the measured visibility by considering the idealized interferometer sketched in Figure 1. In the left panel of this figure, an optical interferometer is represented as a Young's two-slit experiment (Born & Wolf 1965). Flat wavefronts from a distant source impinge on the slits and produce an interference pattern on an illuminated screen; this interference pattern drawn corresponds to the field *intensity*, not the electric field strength.

The spatial frequency of these (intensity) fringes is determined by the distance between the slits (in units of the wavelength of the illuminating radiation). However if the pathlength above one slit is changed (due to a pocket of warm air moving across the aperture, for example), the interference pattern will be shifted by an amount depending on the difference in pathlength of the two legs in this simple interferometer. If the extra pathlength is half the wavelength, the fringe pattern will shift by half a fringe, or π radians. The phase shift is completely independent of the slit separation, and only depends on slit-specific phase delays.

The loss of this phase information has serious consequences. Imaging of non-centrosymmetric objects rely on the Fourier phase information encoded in the intrinsic phase of interferometer fringes. Without this information, imaging can not be done except for simple objects such as disks or round stars.

1.2 Closure Phase and the Bispectrum

Consider the right panel of Figure 1 in which a phase delay is introduced above telescope 2. This causes a phase shift in the fringe detected between telescopes 1-2, as discussed in the last section. Note that a phase shift is also induced for fringes between telescopes 2-3; however, this phase shift is equal but *opposite* to the one for telescopes 1-2. Hence, the sum of three fringe phases, between 1-2, 2-3, and 3-1, is insensitive to the phase delay above telescope 2. This argument holds for arbitrary phase delays above any of the three telescopes. In general, the sum of three phases around a closed triangle of baselines, the *closure phase*, is a good interferometric observable; that is, it is independent of telescope-specific phase shifts induced by the atmosphere or optics.

The idea of closure phase was first introduced to compensate for poor phase stability in early radio VLBI work (Jennison 1958). Application at higher frequencies was first mentioned by Rogstad 1968, but only much later carried out in the visible/infrared through aperture masking experiments (Baldwin *et al.* 1986; Haniff *et al.* 1987; Readhead *et al.* 1988). Currently only three separate-element interferometers have succeeded in obtaining closure phase measurements, in the optical (visible/infrared), first at COAST (Baldwin *et al.* 1996), soon after at NPOI (Benson *et al.* 1997), and most recently at IOTA in 2002.

Another way to derive the invariance of the closure phase to telescope-specific phase shifts is through the *bispectrum*. The bispectrum $\tilde{B}_{ijk} = \tilde{V}_{ij}\tilde{V}_{jk}\tilde{V}_{ki}$ is formed through triple products of the complex visibilities around a closed triangle, where ijk specifies the three telescopes. The bispectrum is a complex quantity whose phase is identical to the closure phase (the amplitude of the bispectrum is often referred to as the *triple amplitude*). The use of the bispectrum for reconstructing diffraction-limited images was developed independently (Weigelt 1977) of the closure phase techniques, and the connection between the approaches realized only later (Roddier 1986; Cornwell 1987).

For N telescopes, there are “ N choose 3” $\binom{N}{3} = \frac{(N)(N-1)(N-2)}{(3)(2)}$, possible closing triangles. However, there are only $\binom{N}{2} = \frac{(N)(N-1)}{2}$ independent Fourier phases; clearly not all the closure phases can be independent. The number of *independent* closure phases is only $\binom{N-1}{2} = \frac{(N-1)(N-2)}{2}$, equivalent to holding one telescope fixed and forming all possible triangles with that telescope. The number of inde-

Table 1. Phase information contained in the closure phases alone

Number of Telescopes	Number of Fourier Phases	Number of Closing Triangles	Number of Independent Closure Phases	Percentage of Phase Information
3	3	1	1	33%
7	21	35	15	71%
21	210	1330	190	90%
27	351	2925	325	93%
50	1225	19600	1176	96%

pendent closure phases is always less than the number of phases one would like to determine, but the *percent* of phase information retained by the closure phases improves as the number of telescopes in the array increases. Table 1 lists the number of Fourier phases, closing triangles, independent closure phases, and recovered percentage of phase information for telescope arrays of 3 to 50 elements. For example, approximately 90% of the phase information is recovered with a 21 telescope interferometric array (e.g., Readhead *et al.* 1988). This phase information can be coupled with other image constraints (e.g., finite size and positivity) to reconstruct the source brightness distribution.

1.3 Simple Example: a Binary

Let us start by analyzing a simple case and one which is scientifically relevant. How do the closure phases behave for a binary?

Since the closure phases are independent of the phase center, one can strategically place the origin in order to more easily determine the Fourier phases for a given brightness distribution. For example, consider the equal binary system depicted in Figure 2. The complex visibility can be easily written by choosing the origin midway between the two components. Note the abrupt phase jump when the visibility amplitude goes through a null. These discontinuities are smoothed out when the two components are not precisely equal.

But what about the closure phases? Since a closure phase is simply a sum of three phases, we can immediately see that all the closure phases must be either 0° or 180° . In fact, this is true not just for equal binaries, but *any point-symmetric brightness distribution*. This is easily proven: by placing the origin (phase center) at the location of point-symmetry, we can make the imaginary part of the Fourier transform disappear (i.e., all odd basis functions must be zero). Hence, the phases

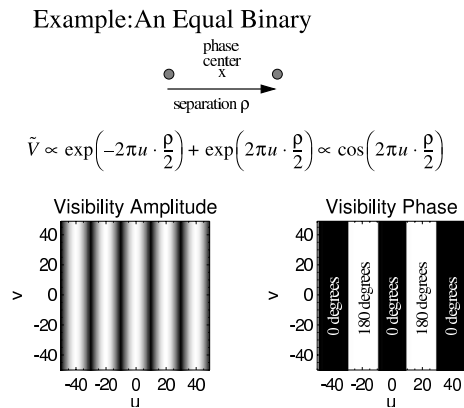


Fig. 2. This figure shows the complex visibility for an equal binary system. With the above choice for the phase center, the Fourier phases can be represented simply. Notice the abrupt phase jumps when visibility amplitude goes through a null.

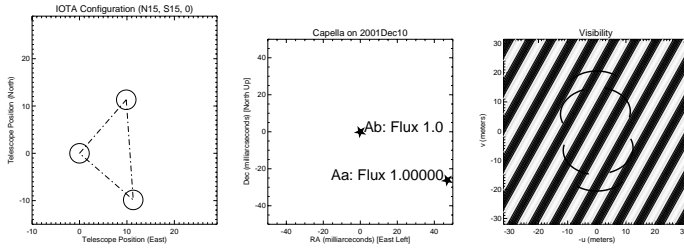


Fig. 3. The left panel shows the telescope positions used for calculating the visibility and closure phase signal of the binary geometry shown in the center panel. The right panel shows the binary visibility pattern projected onto the uv-plane, with the observing (u,v)-tracks marked (6 hours of observing around transit). All the example plots of this section (next two figures) will use this same geometry.

of *all* Fourier components must be either 0° or 180° (the bispectrum is real).

For an equal binary then, we would expect to see abrupt closure phase jumps between 0° and 180° if one of the baselines traverses a null in the visibility pattern. A textbook example (from NPOI) of this behavior is reported in Benson *et al.* (1997). One can determine the binary separation (and brightness ratio) from the closure phase information alone.

How would this look to an interferometer? Figure 3 shows an example interferometer layout (here modelled for IOTA). Figures 4 & 5 show the visibilities and closure phases that would be measured for binaries with different brightness ratios. It is not surprising that the “nearly equal” binary case shown on the right panels of Figure 4 resemble the pattern for the equal binary case (left panels), except the abrupt 180° transitions are now smoothed over, and the closure phase does not quite reach 180° anymore.

Figure 5 explores the consequences for the unequal binary case. We see that

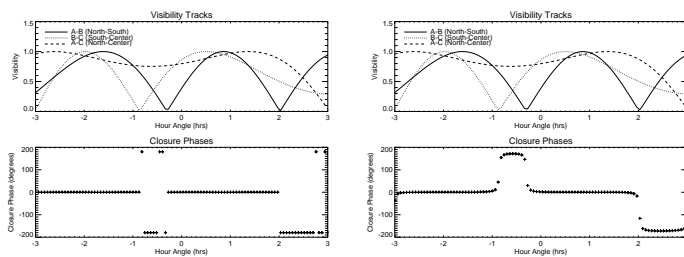


Fig. 4. The left panels shows the visibility data (top) and closure phases (bottom) of an equal binary during the observations described in Figure 3. The right panels show the same for a slightly unequal binary (1 to 1.05). Note how the closure phases smoothly change from 0° to nearly 180° as you would expect for a “nearly” point-symmetric object.

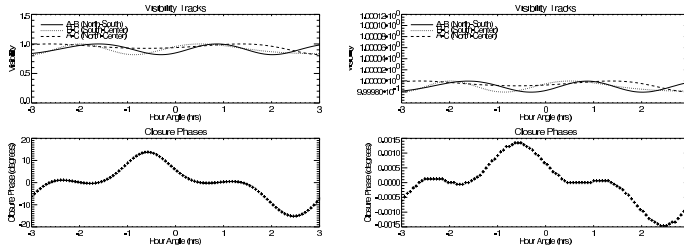


Fig. 5. Same as last figure, but for very unequal binaries. The left panels shows the visibility data (top) and closure phases (bottom) for a binary with flux ratio of 10. The right panels shows the same binary, but for a flux ratio of 100000 (which might be reasonable for a planet). Note that the magnitude of the closure phase signal is of the same order of magnitude (in radians) as the flux ratio, 1×10^{-5} .

the magnitude of the closure phase (in radians) is roughly equal to the “amount” of asymmetry, which for a binary star is equal to the brightness ratio. It is clear that with sufficiently sensitive closure phase measurements, very high contrast binaries could be detected and characterized.

1.4 Related Quantities

1.4.1 Differential Closure Phase

The use of “Differential Phase” is discussed elsewhere in this volume (Stee), where the concept is to calibrate for the atmospheric phase delays in the interferometer by measuring the fringe phases as a function of wavelength. This technique is potentially very powerful, but is subject to uncertainties in the atmospheric dispersion when used over a wide bandpass.

“Differential Closure Phase” refers to measurements of the closure phases at one wavelength relative to another one. The closure phase might be better calibrated by using multi-wavelength measurements, since a “relative” closure phase might be stable to a variety of systematic errors (such as long term drifts in the optics). In addition, the closure phase is more immune to the uncertainties in dispersion, and so could be used for many of the same applications planned for “differential phase,” such as finding planets. Some recent discussion on this can be found in Segransan *et al.* (2000).

1.4.2 Closure Differential Phase

Unfortunately, one limitation of differential phase (and differential closure phase) is that it requires some assumptions about the source structure you are observing. For instance, if one measures the fringe phase in a spectral line compared to the surrounding continuum, one must know *a priori* the intrinsic fringe phase of the continuum in order to interpret the “differential phase.” If the continuum source

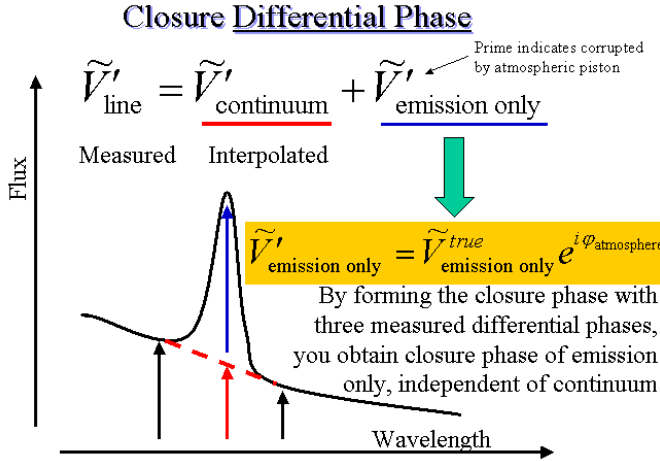


Fig. 6. This figure illustrates the idea behind *closure differential phase*. Using this method, the closure phase of the emission component can be separated from the closure phase of the (arbitrarily complicated) continuum.

is expected to be unresolved, then one can safely assume the continuum fringe phase is zero and there is no problem.

However, consider observing an infrared emission line formed in a jet around a young stellar object. One would expect the near-infrared continuum to have significant contributions from dust scattering and possibly even dust thermal emission. Thus, one can not assume the continuum is unresolved. Further, one might expect the emission to be fairly complicated in morphology, thus the differential phase measured in the spectral line will be difficult to interpret. One would have to first make a continuum image, a difficult task with only three telescopes.

However, Figure 6 introduces a neat idea: the Closure Differential Phase. For each of the three baselines, one can measure the complex visibility in the emission line and in the neighboring continuum. By subtracting these complex quantities, one can isolate the complex visibility of the emission component, albeit corrupted by the atmospheric delay. However, one can form the closure phase using this differential phase measurement, and thus measure the closure phase of the emission component independent of the continuum. The forming of the closure phase using a kind of differential phase motivates the name “closure *differential phase*.” Note that this differential phase is not the traditional differential phase, but rather results from the differencing of the complex visibilities in and out of the line, *not* merely differencing the fringe phases. Since the spectral line emission might be simpler than the continuum, for example in a jet, this method could be potentially useful when it is not feasible to make an image of the continuum.

2 Precision Interferometry with Closure Phases

The precision of measured visibility amplitudes is usually limited by calibration of changing atmospheric conditions. Because the closure phase is largely independent of atmospheric seeing, it is possible that closure phases will be measured with a greater precision than has been possible for visibility amplitudes. Thus model parameters for simple sources could be vastly improved by using well-calibrated closure phases.

Of course, not all simple sources have significant closure phase signals. For instance, the closure phases of a limb-darkened disk only vary across visibility nulls, thus closure phases are useless for precision measurements of limb-darkening. However, there are a number of simple sources which do lend themselves to modeling of the closure phases:

- Non-equal binary stars can be measured using precise closure phases. The separation, brightness ratio and even component diameters can be extracted from the closure phase measurements. High signal-to-noise techniques could allow binaries with large brightness ratios to become detectable using interferometry, perhaps enough to detect some planets.
- While pulsating single stars do not have a time-changing closure phase signal (except beyond the first null), a pulsating star in a binary system will. For instance, a Cepheid changing size and brightness in a binary system could be measured using the time-changing closure phases.
- With good interferometer sensitivity, one could observe crowded fields. The closure phases could help immensely in performing narrow angle astrometry of the various components, and could be used to study dynamics and proper motions.

3 Qualitative Astrophysics with Closure Phases

In the infrared, many targets will have significant contributions from dust shells which may be clumpy, complicated, and not representable by a simple model (we will see). Without good imaging capability, why should we observe such sources with just a 3-telescope interferometer?

Closure phases can discover qualitatively new information about some objects, much like measuring the polarization. Also as for polarization, the result will likely be, as they say, “informative, but not unambiguous.” In this section, I will discuss how to use closure phase measurements with a 3-telescope array to discover fundamentally new things about your target. In this case, I will use the prototypical case of a “dust shell + star” as illustrated in Figure 7.

There are four different kinds of closure triangles you might imagine employing to probe different aspects of this source. These are listed and described in Figure 8.

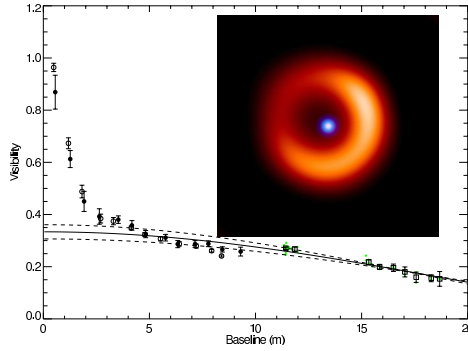


Fig. 7. A common case encountered in infrared interferometry is a star surrounded by a dust shell. This figure shows an example image and corresponding visibility curve. The important point is that the short baselines are probing the large scale structure of the object (the dust shell), while the long baselines resolve out the dust and only “see” the underlying star.

Four Kinds of Useful Closure Triangles for the “Dust Shell + Star” Prototype

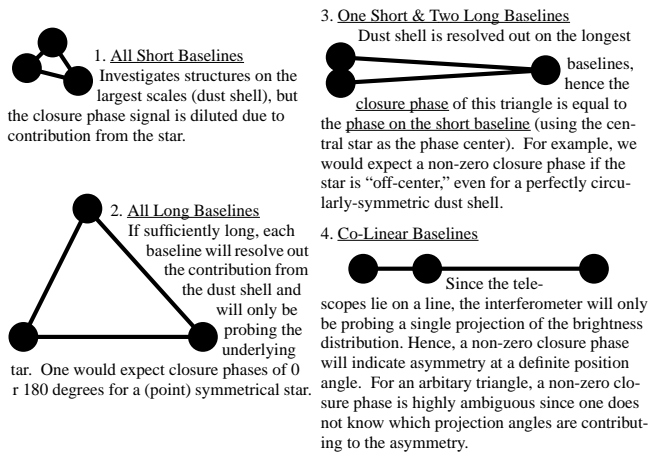


Fig. 8. This figure explain four important kinds of closure triangles.

3.0.3 Implications

Depending on your science goals, you would employ different triangles for your observations. Here are some examples:

1. Goal: Find “interesting” young stellar objects for the subject of an intensive series of observations meant to image the accretion disks. Since YSO disks are pretty small (<5 mas), I would survey a large number of targets with

relatively long baselines. Since “interesting” structure often means “asymmetric” structure, I would use a large equilateral triangle to look for any kind of asymmetry. When we do find something, we will have no idea which axis is asymmetric, but would follow it up (see next entry).

- Goal: We already know an interesting target, and we want to see if the asymmetry is related to other known properties of the system. If you have some idea that one particular axis might be asymmetric (e.g., direction of a previously-seen jet, bi-polar outflow, or a known companion), then set up some linear arrays to probe the different position angles to (dis)prove that the asymmetries are related to these directions. Note that earth rotation will rotate your linear array through a range of position angles and so will not necessarily require many configuration changes (telescope relocations).

3.1 Examples

In Figures 9 & 10, we show examples of visibilities and closure phases based on actual results from aperture masking (Tuthill *et al.* 2001; Danchi *et al.* 2001). The large number of data points were made possible by masking the Keck Telescope (Tuthill *et al.* 2000), and allowed images to be reconstructed. Note the bottom left panel shows all the closure phases plotted against the longest baseline length in the corresponding closure triangle. In such a plot, one expects near-zero closure phases until there is enough resolution (long enough baselines) to resolve any asymmetric

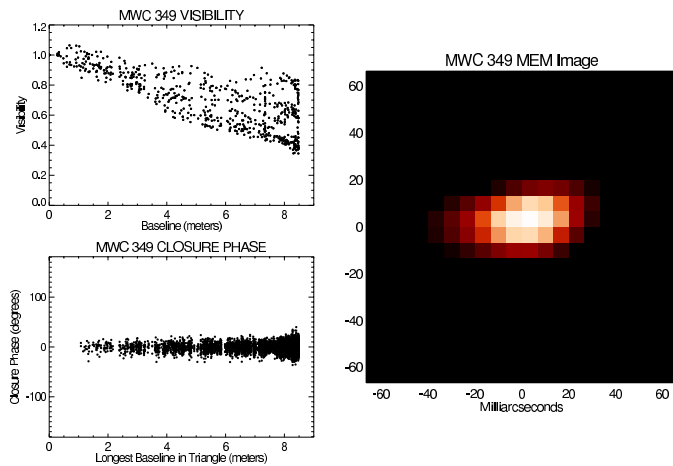


Fig. 9. This figure shows actually measured visibilities and closure phases for the young stellar object MWC 349. One can see directly from the visibilities that the source is highly elongated. However, the small (near zero) closure phases show the source is point-symmetric. Even without imaging (right panel), we could have guessed this source would look like a symmetric edge-on disk.

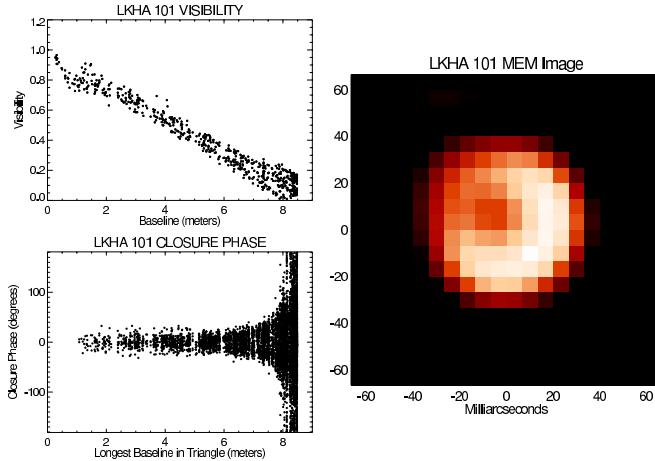


Fig. 10. This figure shows actually measured visibilities and closure phases for the young stellar object LkH α 101. One can see directly from the visibilities that the source is not highly elongated in any single direction. However, the large closure phases measured in triangles with long (>7 m) baselines show that there is highly asymmetric structure on small scales. The right hand panel shows the reconstructed image, which is indeed consist with these qualitative features: a bright dust ring which is brighter on one side.

structure present. We analyze the data for each source in the corresponding figure captions.

3.2 YSO disks with realistic interferometer

Figure 11 shows how a realistic three-telescope interferometer such as IOTA would see a young stellar object. This YSO model was based on the LkH α 101 disk seen in Figure 10, but shrunk in size by a factor of 7. The closure phases for smaller triangles are all near zero degrees and the visibility amplitudes do not show a strong dependence with position angle. The information about the asymmetric disk emission is only clearly seen in the closure phases measured with the longest baselines.

4 Imaging with Closure Phases

There is no space in this short chapter to discuss strategies for imaging with closure phases. This topic was touched on by Chris Haniff in an earlier chapter, and we refer the interested reader to his excellent introduction. For more discussion on self-calibration and the use of closure phases in image reconstruction, please consult Readhead & Wilkinson (1978), Cornwell & Wilkinson (1981), & Monnier (1999, 2000, and references therein).

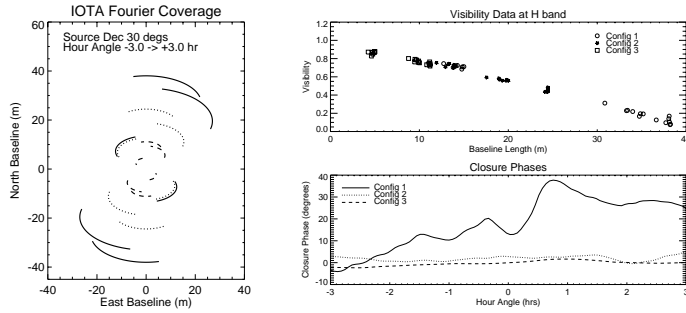


Fig. 11. This figure shows the simulated results of observing a source like LkH α 101 using IOTA. The (u,v)-coverage for three different baseline triangles are shown, as are the visibilities and closure phases covering a range of hour angles. Only “Config 3,” the longest baseline configuration, shows non-zero closure phases and deviations from circular symmetry. This is a warning: it will be easy to jump to the wrong conclusions when observing these kinds of sources with insufficient Fourier Coverage.

5 Conclusions

For simple sources, closure phases from three-telescope arrays promise to produce the most precisely calibrated quantities in optical interferometry. The ultimate precision will probably be limited by our ability to calibrate systematic errors that we have not even discovered yet. For more complicated sources, even limited closure phase measurements can yield important astrophysical discoveries, preceding the capabilities for full imaging. There is much to be done.

I recognize interesting and thought-provoking discussions with Chris Haniff, Dave Buscher, and John Young on various aspects of closure phase measurement and imaging theory during this meeting. In particular, the idea of “closure differential phase” emerged from a discussion with Dave Buscher about Carla Gil’s proposed observations of jets around young stars using the AMBER instrument on VLTI.

References

- Baldwin, J. E., Haniff, C. A., Mackay, C. D., & Warner, P. J. 1986, *Nature*, 320, 595
 Baldwin *et al.* 1996, *A&Ap*, 306, L13
 Benson *et al.* 1997, *AJ*, 114, 1221
 Born, M. & Wolf, E. “Principles of optics.” 1965 (3rd ed)
 Cornwell, T.J. & Wilkinson, P.N. 1981, *MNRAS*, 196, 1067
 Cornwell, T. J. 1987, *A&Ap*, 180, 269
 Danchi, W. C., Tuthill, P. G., & Monnier, J. D. 2001, *ApJ*, 562, 440
 Haniff, C. A., Mackay, C. D., Titterton, D. J., Sivia, D., & Baldwin, J. E. 1987, *Nature*, 328, 694
 Jennison, R. C. 1958, *MNRAS*, 188, 276

- Monnier, J.D. 1999, Ph.D. Thesis, University of California at Berkeley
- Monnier, J.D. 2001, Chapter 13 in *Principles of Long Baseline Stellar Interferometry* (ed. by P. Lawson), JPL Publications
- Readhead, A.C.S. & Wilkinson, P.N. 1978, ApJ, 223, 25
- Readhead, A.C.S. *et al.* 1988, AJ, 95, 1278
- Roddier, F. 1986, Opt. Comm., 60, 145
- Rogstad, D. H. 1968, App. Opt., 7, 585
- Segransan, D., Beuzit, J., Delfosse, X., Forveille, T., Mayor, M., Perrier-Bellet, C., & Allard, F. 2000, Proc. of SPIE, 4006, 269.
- Tuthill, P. G., Monnier, J. D., Danchi, W. C., Wishnow, E. H., & Haniff, C. A. 2000, PASP, 112, 555
- Tuthill, P. G., Monnier, J. D., & Danchi, W. C. 2001, Nature, 409, 1012
- Weigelt, G. P. 1977, Opt. Comm., 21, 55